Digest Journal of Nanomaterials and Biostructures Vol. 20, No. 4, October-December 2025, p. 1499-1506

`

Synthesis and characterization of novel sulfanilic acid-based metal-organic frameworks for biological applications

A. Batool [a], A. Javaid [a], S. Haq [b,*], M. U. Sadiq [c], M. Ben Ali [d], Sh. Rasulov [b], Z. U. Rehman [e], A. Hedfi [d], A. Shah [f]

[a] *Department of Chemistry, University of Azad Jammu and Kashmir, Muzaffarabad 13100, Pakistan*

[b] *Institute of Fundamental and Applied Research, National Research University TIIAME, Kori Niyoziy 39, Tashkent 100000, Uzbekistan*

[c] *Department of Chemistry, Quiad Azam University, Islamabad Pakistan.*

[d] *Department of Biology, College of Sciences, Taif University, PO Box 11099, Taif 21944, Saudi Arabia*

[e] *Institute for Advanced Materials, College of Materials science & Engineering, Jiangsu University, P.R. China*

[f] *Department of Microbiology, Hazara University, Mansehra, KP, Pakistan*

The alarming rise in antibiotic-resistant bacteria and oxidative stress-related diseases has created an urgent need for novel therapeutic therapies. Metal-organic frameworks, known for their tunable structure and biological properties have emerged as promising candidates for combating antimicrobial resistance and oxidative stress. In this study, two MOFs were synthesized using nickel and copper as metal centers coordinated with sulfanilic acid as an organic linker. The synthesized MOFs were analyzed using fourier transform, scanning electron microscopy, and energy dispersive X-ray spectroscopy. The antibacterial efficacy of prepared MOFs was evaluated using the agar well diffusion method against *S. aureus* and *E. coli*, while their antioxidant potential was evaluated using ABTS assay. Cu-MOF showed superior antibacterial potential, especially against *E. coli*, and exhibited higher antioxidant activity with IC_{50} of 23.29 µg/µL. The findings of this work suggest that both Cu-MOF and Ni-MOF have potential as effective antibacterial and antioxidant agents, with Cu-MOF showing superior efficacy in both domains.

(Received October 10, 2024; Accepted December 8, 2025)

Keywords: Copper, Nickel, Metal-organic frameworks, Antibacterial, Antioxidant

1. Introduction

The rise of antibiotic-resistant bacteria and the growing prevalence of oxidative stress-related diseases have rendered current treatments ineffective leading to increasing mortalities. It is anticipated that by 2050, the number of fatalities caused by antimicrobial resistance (AMR) might reach 10 million, and cause a staggering burden of up to USD 100 trillion on the world economy, resulting in extreme poverty for 28 million people. Furthermore, the World Health Organization declared AMR among the top ten health hazards [1]. Similarly, oxidative stress can cause cell damage and lead to severe fatal diseases including cancer, neurodegenerative, and cardiovascular disorders [2]. To counter these fatal threats, it is crucial to develop novel, efficient, and economical materials capable of antioxidant and antibacterial potential [3]. Recent significant advancements in nanotechnology have opened new avenues for addressing these issues. Nanomaterials are known for their excellent biological potential without creating microbial resistance and oxidative stress and have gained significant attention in this field [4]. Consequently, a variety of nanomaterials particularly metal oxide nanoparticles, metallic nanoparticles, metal-organic frameworks (MOFs), and, polymers have been prepared and employed as antimicrobial as well as antioxidant agents.

* Corresponding author: cii_raj@yahoo.com
https://doi.org/10.15251/DJNB.2025.204.1499

Among different types of investigated nanomaterials, MOFs have gained significant importance as an antioxidant as well as antibacterial agents [5].

MOFs are highly porous coordination molecules formed by the coordination/ combination of an organic linker with metal ions [6]. Due to their exceptional surface area, flexible functionalization strategies, and tunable pore size MOFs have been widely studied in different fields, including biological, energy, and gas storage applications [7]. Recently, MOFs have received significant attention in biological fields, particularly for their potential as antioxidant and antimicrobial agents [8]. The enhanced activity of MOFs can be related to the intrinsic biological potential of metal ions and organic linkers. Therefore, we aim to synthesize two MOFs comprising of nickel and copper as metal ions and sulfanilic acid as the organic linker [9].

Sulfanilic acid is a bidentate ligand and is a promising candidate for the synthesis of MOFs due to functional groups (sulfonic and amine groups). Sulfanilic acid contains a sulfonic group (-SO_3H) and an amine group (-NH_2), which offer multiple coordination sites for the binding of metal ions, enhancing the versatility of resulting MOFs. The -SO_3H group is highly polar and acts as a strong electron donor, forming a stable bond with metal centers such as Cu^{2+}, Zn^{2+}, and Fe^{3+}, while -NH_2 offers an additional site for coordination and potential for post-synthetic modifications. Furthermore, the rigid benzene ring in the sulfanilic acid provides structural rigidity, ensuring the formation of a robust, crystalline framework.

In this work, we synthesized MOFs consisting of nickel and metal centers linked with sulfanilic acid as an organic linker. The functional, morphological, and elemental analysis was performed using FTIR, SEM, and EDX analysis. The prepared MOFs were subjected to antioxidant and antimicrobial assays, revealing their potential utilization in the biomedical field.

2. Experimental

2.1. Chemicals

Copper sulfate pentahydrate ($CuSO_4 \cdot 5H_2O$), nickel nitrate hexahydrate ($NiNO_3.6H_2O$), 2,2'-azinobis-(3-ethylbenzothiazoline-6-sulfonic acid) (ABTS), potassium persulphate, sulfanilic acid, and methanol of high purity were used in this work. During this research work, all the working solutions were made using distilled water.

2.2. Synthesis of Cu (II) based MOF (MOF-1)

For the preparation of MOF-1, 1.24 g of $CuSO_4 \cdot 5H_2O$ and 0.865 g of sulfanilic acid were separately solubilized in distilled water. Both the solutions were mixed and transferred to a 100 mL round bottom flask. The solution was then heated under reflux conditions for 14 h. After heating, the mixture was allowed to cool at ambient conditions. After being washed with distilled water, the solid product was dried in an oven at 100 °C to create a powder.

2.3. Synthesis of Ni (II) based MOF (MOF-2)

A similar approach was used for the preparation of Ni (II) based MOF. For this purpose, 1.45 g of $NiNO_3.6H_2O$ and 0.865 g of sulfanilic acid were dissolved in distilled water individually. After complete solubilization, both solutions were mixed and transferred to a 100 mL round bottom flask, and the solution was heated for 14 hours while being refluxed. After the reflux period, the solution was allowed to cool to ambient temperature. To produce dry powder, the resulting product was washed with distilled water and heated at 100 °C.

2.4. Characterization

The physicochemical properties of synthesized sulfanilic acid based-MOFs were studied utilizing several techniques such as SEM, FTIR, and EDX to analyze the functional groups present in the prepared MOFS, morphology, and elemental composition.

2.5. Biological activities of synthesized MOFs

2.5.1 Antibacterial assay

The antibacterial properties of prepared MOFs were tested against selected bacterial species with the help of the agar well diffusion method [10]. Pathogenic bacteria cultured on a nutrient broth medium were utilized to inoculate the agar surface by distributing the microbial inoculum evenly throughout the whole surface. Using a sterile 1ml micropipette, three wells (8-10 mm in diameter) were created in the agar layer. The well was filled with 30 µL of known concentration of MOF suspensions and a standard drug (ciprofloxacin). Then the agar plate was incubated at 37 °C for 18-20 h. The diameter of the inhibitory zones was measured after the specific duration. This procedure was repeated for different concentrations of MOFs.

2.5.2 Antioxidant assay

To investigate the ability of different concentrations of synthesized MOFs to detoxify free radicals, an ABTS radical cation ($ABTS^{\cdot+}$) assay was conducted. $ABTS^{\cdot+}$ assay is a widely adopted method to assess the ability of different antioxidant substances. For this purpose, $ABTS^{\cdot+}$ was generated by reacting 5 mM potassium persulfate with 14 mM ABTS. The resulting stock solution was incubated in the dark for 16 hours. After this, the dilution of $ABTS^{\cdot+}$ solution was carried out using distilled water to adjust absorbance to 2.50 ± 0.05 at 734 nm. Absorbance of $ABTS^{\cdot+}$ solution was measured which acts as control (A_o). Different concentrations of synthesized MOFs were prepared by adding each concentration to 1 ml of distilled methanol and subsequently sonicating. An aliquot of 50 µL of each sample was taken in different test tubes to which 1 mL of $ABTS^{\cdot+}$ solution was added. The mixture was shaken and incubated in the dark for 30 minutes. The absorbance of the reaction (Ai) was recorded. The following formula was used for calculating the percent radical scavenging activity (% RSA) [11].

$$\%RSA = \left(\frac{A_o - A_i}{A_o}\right) \times 100 \quad (1)$$

3. Results and discussion

Figure 1A depicts the FTIR spectrum of Cu-MOF (MOF-1), which shows a broad flat band around 3750 cm^{-1} to 3000 cm^{-1}. This band is indicative of O-H and N-H stretching vibrations of the amine and hydroxyl groups [12,13]. A peak at 1632 cm^{-1} corresponds to the C=C and C-H stretching vibrations of the aromatic ring, while the peak at 1385 cm^{-1} is likely due to the stretching vibration of the C-N bond in sulfanilic acid. A band in the 1250–1000 cm^{-1} range reflects the S=O bonds stretching vibrations confirming the presence of the sulfonic acid group [14]. Finally, the peaks in the 600- 400 cm^{-1} are attributed to the Cu-N bond or Cu-O stretching vibration, confirming the biding of Cu with organic linker and successful formation of Cu-MOF. In Cu – sulfanilic acid MOF, the metal atom can be coordinated with the nitrogen atom of the amine group as well as with the oxygen of sulfonic acid of sulfanilic acid [15].

Figure 1B presents the FTIR spectrum of MOF-2 (Ni-MOF), which shows a broad peak in 3812 – 3000 cm^{-1} originating from O-H and N-H stretches [16,17]. C=C or C-H stretching vibration of the benzene ring is observed at 1639 cm^{-1}. This peak can also be attributable to the C-N bending vibration of the amine group. Similarly, the peak at 1388 cm^{-1} could be due to the stretching vibration of the C-N bond of sulfanilic acid. Three less intense peaks at 1200 –1o00 cm^{-1} region are likely due to symmetric and asymmetric stretching of the S=O bonds of the sulfonic group, which indicates the retention of sulfonic group in the prepared MOF. The peak at 520 cm^{-1} can be ascribed to the Ni-O or Ni-N stretching, indicating the formation of metal-ligand bonds between nickel atoms and sulfanilic acid in the MOF structure [15].

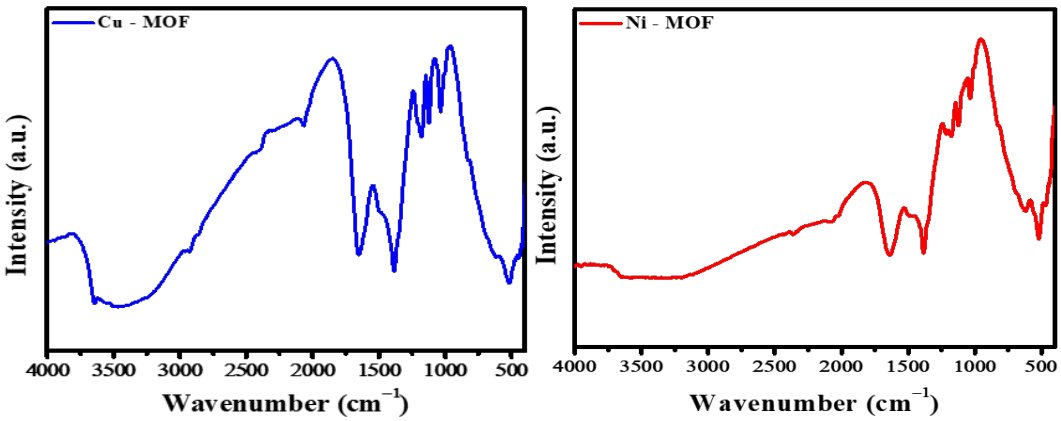

Fig. 1. FTIR spectrum of (A) Cu-MOF and (B) Ni-MOF.

SEM micrographs of Cu-MOF are displayed in Figures 2A and B, which show rough and irregular structures comprising of various plate-like and granular morphologies. The rough and uneven surface indicates the presence of a porous structure. Various cavities with different shapes and sizes are present in the network. The EDX study was performed to visualize the composition of Cu-MOF, which is presented in Figure 2C. EDX spectrum shows a dominant peak of Cu at 1 keV, along with two smaller peaks at 8 keV and 9 keV, corresponding to the highest atomic percentage of 64.21% and weight percentage of 28.90%. Additionally, the spectrum displays well-defined peaks for C at 0.1 keV and O at 0.2 keV, with weight percentages of 28.61% and 42.29%, and atomic percentages of 12.02% and 23.77%, respectively.

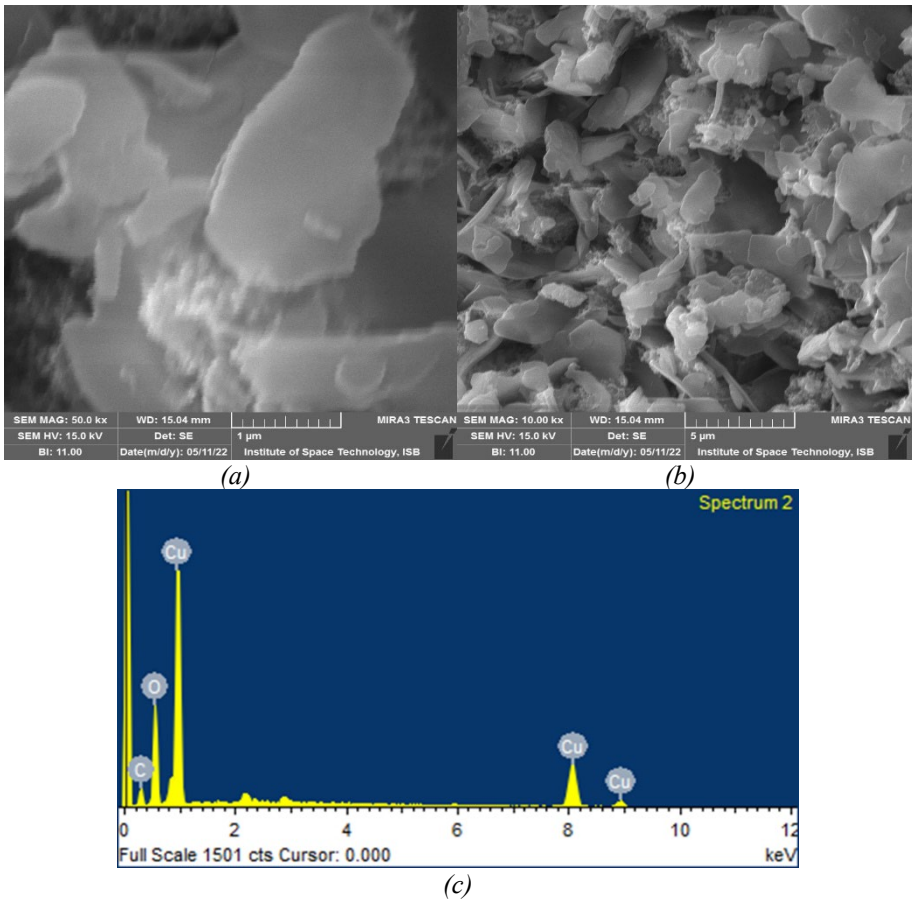

Fig. 2. (A, B) SEM analysis of Cu-MOF at low and high magnification and (C) EDX spectrum of Cu-MOF.

SEM micrographs of Ni-MOF are presented in Figure 3A and B. The particles are randomly arranged to form porous structures, as seen in the less-magnified SEM image. The particles merged together to form a flat surface, but in most cases, the particles seemed to have their individual boundaries. Figure 3B shows the highly fibrous texture of Ni-MOF suggesting a highly porous and intricate structure. The fine thread-like structures indicate high surface area and porosity which are typical properties of MOFs. The elemental composition of Ni-MOF was also studied, which shows the highest percentage of nickel having 39.52% by weight percent and 15.27% by atomic percent (Figure 3C). The peaks for carbon, nitrogen, oxygen, sodium, sulphur, and potassium appeared at 0.1 keV and 0.2 keV, having weight percent 11.90%, 2.80%, 36.62%, 0.89%, 0.87%, and 7.40% and atomic percent of these elements are 22.48%, 4.53%, 51.93%, 0.88%, 0.62%, and 4.29% respectively. All these peaks show that all the desired elements are present in the sample which shows the successful preparation of MOF.

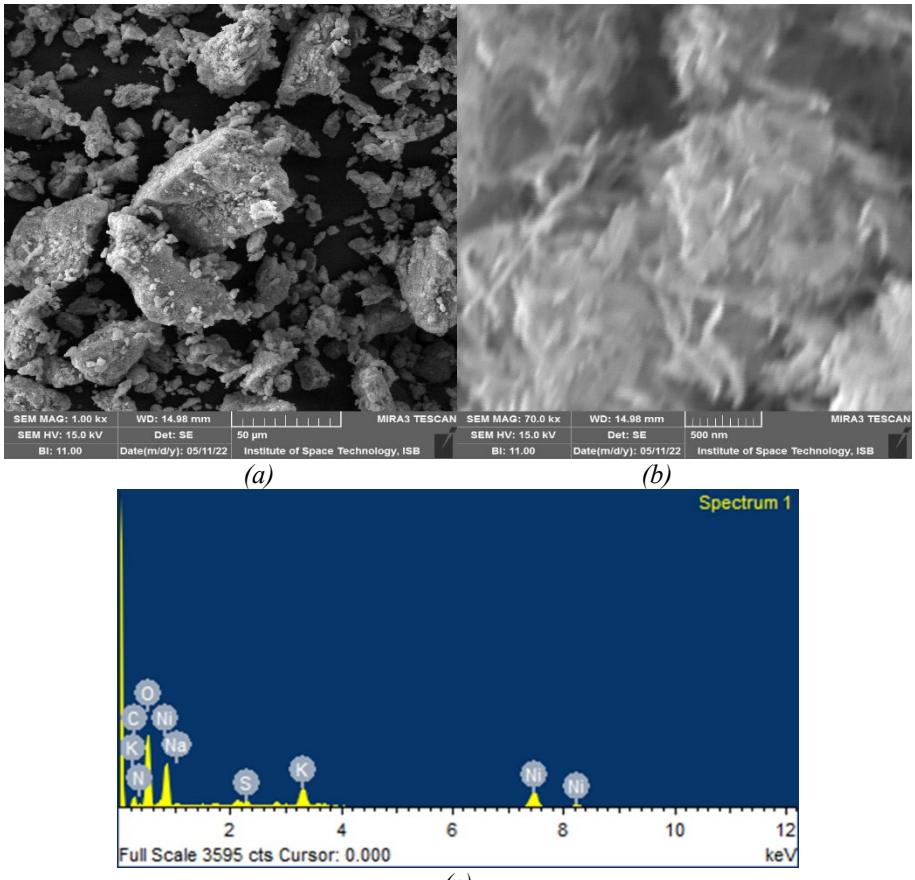

Fig. 3. (A, B) SEM analysis of Cu-MOF at low and high magnification and (C) EDX spectrum of Cu-MOF.

3.1. Antibacterial activity

The agar well method was used to investigate the antimicrobial efficiency of Cu-MOF and Ni-MOF against *S. aureus* and *E. coli*. As presented in Figure 4, Cu-MOF demonstrated robust efficacy against *E. coli* with 10 mm ZOI, and less effect against *S. aureus* with 7 mm ZOI. Similarly, Ni-MOF exhibited moderate activity against *S. aureus* with a zone of inhibition of 6 mm, while it exhibited stronger activity against *E. coli* with a ZOI of 9 mm.

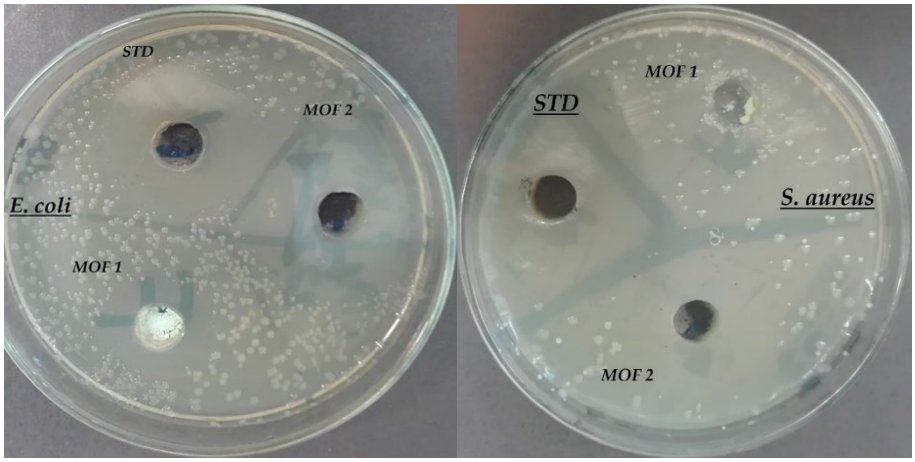

(a) (b)

Fig. 4. Antibacterial efficacy of MOF-1 and MOF-2 against (A) E. coli and (B) S. aureus.

The antibacterial effect of MOF-1 (Ni-MOF) and MOF-2 (Cu-MOF) can be ascribed to the release of Ni^{2+} and Cu^{2+}, which can generate the reactive oxygen species. These species induce oxidative stress, leading to damage of bacterial proteins, lipids, and DNA. The higher antimicrobial effect of both MOFs against *E. coli* can be linked to the bacterial cell wall structure. *S. aureus* has a thick layer of peptidoglycan but lacks an outer membrane, while the outer membrane of *E. coli* is composed of a thin peptidoglycan layer with an inner membrane of lipopolysaccharide. The outer membrane provides resistance to antimicrobial agents, but once it is damaged, *E. coli* becomes highly susceptible to damage. Ni^{2+} and Cu^{2+} can interact with lipopolysaccharide and destabilize it, allowing the greater penetration of Ni^{2+} and Cu^{2+} into periplasmic space and cytoplasm. Once the outer membrane is damaged, the *E. coli* become more susceptible to Ni^{2+} and Cu^{2+} induced oxidative stress and enzymatic disruption. While the peptidoglycan layer of *S. aureus* is dense and highly cross-linked providing rigidity and protection against external stress. Ni^{2+} and Cu^{2+} may have a harder time penetrating the thicker peptidoglycan layer, which might reduce the efficiency of Ni-MOF and Cu-MOF as compared to *E. coli* [7,18].

3.2. Antioxidant activity

In the human body, free radicals are produced as a byproduct of metabolic processes or they may be produced due to exposure to radiation, pollution, cigarette smoke, and toxins. These free radicals cause oxidative stress leading to severe diseases such as Parkinson's, Alzheimer's, diabetes, arthritis, and cardiovascular diseases. Antioxidants can help to slow down the progression of diseases associated with oxidative stress.

In this work, the antioxidant potential of Cu-MOF and Ni-MOF was assessed using ABTS assay. It can be seen in Figure 5 that the antioxidant efficiency of prepared MOFs increased with increasing dose. Among the two tested MOFs, the maximum inhibitory effect was found at 100 µg/µL for Cu-MOFs (83.68%) followed by 100 µg/µL of Ni-MOF (79.05%). The IC_{50} value was calculated using the linear calibration curves, which were 40.27 for Ni-MOF and 23.29 for Cu-MOF. The lowest IC_{50} for Cu-MOF shows higher efficiency in combating free radicals [19,20].

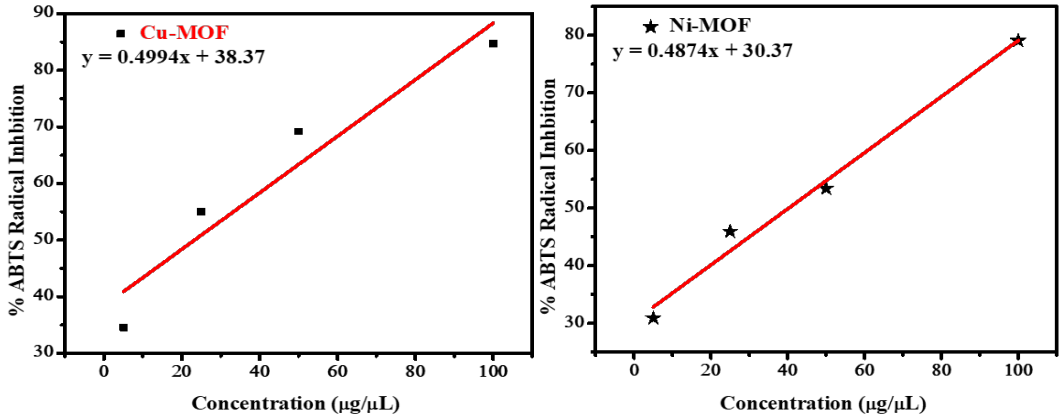

Fig. 5. Linear plot of ABTS radical cation inhibition efficiency of (A) Cu-MOF and (B) Ni-MOF.

4. Conclusion

In this study, two MOFs were successfully synthesized using sulfanilic acid as an organic linker. Both synthesized MOFs were analyzed using FTIR, SEM, and EDX analysis which confirm the synthesis of MOFs. Both MOFs exhibited significant antibacterial and antioxidant activities showcasing their prominent potential in the biological field. The results of antibacterial activity revealed that both MOFs exhibited high antibacterial activity, with Cu-MOF demonstrating a superior efficacy against *E. coli* (ZO1 = 10 mm) compared to *S. aureus* (ZO1 = 7 mm). Similarly, Cu-MOF exhibited higher antioxidant potential with an IC_{50} value of 23.29 µg/µL in comparison to Ni-MOF (40.27 µg/µL). The enhanced performance of Cu-MOF can be ascribed to the efficient release of Cu^{2+} ion and their interaction with bacterial membranes, as well as their ability to scavenge free radicals. These finding suggest that Cu-MOF in particular holds promise as a potential dual-function therapeutic material for combating bacterial infection as well as oxidative stress-related diseases.

Acknowledgments

The authors extend their appreciation to Taif University, Saudi Arabia, for supporting this work through project number (TU-DSPP-2024-158).

References

[1] R. R. Haikal, N. El Salakawy, A. Ibrahim, S. L. Ali, W. Mamdouh, Nanoscale Adv. 4664-4671 (2024); https://doi.org/10.1039/D4NA00519H

[2] E. O. Olufunmilayo, M. B. Gerke-Duncan, R. M. D. Holsinger, Antioxidants 12(2), 1-30 (2023); https://doi.org/10.3390/antiox12020517

[3] M. Kiran, K. A. Yasin, S. Haq, K. Elmnasri, F. Ben Abdallah, M. Ben Ali, A. Shah, A. Hedfi, E. Mahmoudi, Mater. Res. Express 10(10), (2023); https://doi.org/10.1088/2053-1591/acfd0f

[4] M. A. El-Bindary, M. G. El-Desouky, A. A. El-Bindary, Appl. Organomet. Chem. 36(5), 1-16 (2022); https://doi.org/10.1002/aoc.6660

[5] X. Jiang, X. Liu, T. Wu, L. Li, R. Zhang, X. Lu, Talanta 194(967), 591-597 (2019); https://doi.org/10.1016/j.talanta.2018.10.093

[6] B. B. Seyyedi, Metal-Organic Frameworks : A New Class of Crystalline Porous Materials, (2), 123-125 (2015); https://doi.org/10.1595/205651315X687425

[7] R. Roudbari, N. Keramati, M. Ghorbani, J. Mol. Liq. 322(Ii), 114524 (2021); https://doi.org/10.1016/j.molliq.2020.114524

[8] A. A. El-Bindary, E. A. Toson, K. R. Shoueir, H. A. Aljohani, M. M. Abo-Ser, Appl. Organomet. Chem. 34(11), 1-15 (2020); https://doi.org/10.1002/aoc.5905

[9] F. T. Alshorifi, S. M. El Dafrawy, A. I. Ahmed, ACS Omega 7(27), 23421-23444 (2022); https://doi.org/10.1021/acsomega.2c01770

[10] W. Rehman, S. Haq, B. Muhammad, S. F. Hassan, A. Badshah, M. Waseem, F. Rahim, O.-U.-R. Abid, F. L. Ansari, U. Rashid, J. Organomet. Chem. 767, 91-100 (2014); https://doi.org/10.1016/j.jorganchem.2014.05.027

[11] F. Ke, M. Zhang, N. Qin, G. Zhao, J. Chu, X. Wan, J. Mater. Sci. 54(14), 10420-10429 (2019); https://doi.org/10.1007/s10853-019-03604-7

[12] C. Wang, X. Qian, X. An, Cellulose 22(6), 3789-3797 (2015); https://doi.org/10.1007/s10570-015-0754-4

[13] S. Haq, W. Rehman, M. Rehman, J. Inorg. Organomet. Polym. Mater. 30(4), 1197-1205 (2020); https://doi.org/10.1007/s10904-019-01256-3

[14] A. Piri, M. Kaykhaii, M. Khajeh, A. R. Oveisi, BMC Chem. 18(1), 1-14 (2024); https://doi.org/10.1186/s13065-024-01171-w

[15] S. Baik, H. Zhang, Y. K. Kim, D. Harbottle, J. W. Lee, RSC Adv. 7(86), 54546-54553 (2017); https://doi.org/10.1039/C7RA09541D

[16] Y. Zhang, Y. Bin Niu, T. Liu, Y. T. Li, M. Q. Wang, J. Hou, M. Xu, Mater. Lett. 161, 712-715 (2015); https://doi.org/10.1016/j.matlet.2015.09.079

[17] S. Haq, W. Rehman, M. Waseem, J. Inorg. Organomet. Polym. Mater. 29(3), 651-658 (2018); https://doi.org/10.1007/s10904-018-1038-x

[18] M. Mahfooz-Ur-Rehman, W. Rehman, M. Waseem, B. A. Shah, M. Shakeel, S. Haq, U. Zaman, I. Bibi, H. D. Khan, J. Chem. Eng. Data 64(6), 2436-2444 (2019); https://doi.org/10.1021/acs.jced.8b01243

[19] A. Hamid, S. Haq, S. Ur Rehman, K. Akhter, W. Rehman, M. Waseem, S. Ud Din, Zain-ul-Abdin, M. Hafeez, A. Khan, A. Shah, Chem. Pap. 75(8), 4189-4198 (2021); https://doi.org/10.1007/s11696-021-01650-7

[20] J. Aien, A. A. Khan, S. Haq, A. R. Khan, K. Elmnasri, M. Ben Ali, M. S. AL-Harbi, M. I. Alghonaim, S. A. Alsalamah, A. A. Qurtam, F. Boufahja, A. Hedfi, M. Dellali, Crystals 13(2), (2023); https://doi.org/10.3390/cryst13020330